Hypertension Research (2019) 42:1858–1871
https://doi.org/10.1038/s41440-019-0311-x

ARTICLE

Augmented *O*-GlcNAcylation attenuates intermittent hypoxia-induced cardiac remodeling through the suppression of NFAT and NF-κB activities in mice

Takatoshi Nakagawa[1] · Yuichi Furukawa[1,2] · Tetsuya Hayashi[1,2] · Atsuo Nomura[1,2] · Shunichi Yokoe[1] · Kazumasa Moriwaki[1] · Ryuji Kato[2] · Yoshio Ijiri[2] · Takehiro Yamaguchi[3,4] · Yasukatsu Izumi[4] · Minoru Yoshiyama[3] · Michio Asahi[1]

Received: 1 March 2019 / Revised: 4 June 2019 / Accepted: 3 July 2019 / Published online: 13 August 2019

Abstract

Type 2 diabetes mellitus (T_2DM) has been reported to be associated with cardiac remodeling. Although *O*-GlcNAcylation is known to be elevated in diabetic and ischemic hearts, the effects of *O*-GlcNAcylation on cardiac remodeling induced by intermittent hypoxia (IH), such as sleep apnea syndrome (SAS), remain unknown. To evaluate the effects, we induced IH in wild-type (WT) and transgenic *O*-GlcNAc transferase (*Ogt*-Tg) mice. Two weeks of IH increased *O*-GlcNAcylation in the heart tissues of both strains of mice, whereas *O*-GlcNAcylation in *Ogt*-Tg mice was significantly higher than that in WT mice under both normoxic and IH conditions. WT mice exhibited cardiac remodeling after IH, whereas cardiac remodeling was significantly attenuated in *Ogt*-Tg mice. Oxidative stress and apoptosis increased after IH in both strains of mice, whereas the rate of increase in these processes in *Ogt*-Tg mice was significantly lower than that in WT mice. To examine the mechanism of cardiac remodeling attenuation in *Ogt*-Tg mice after IH, the effects of *O*-GlcNAcylation on the activities of the master regulators nuclear factor of activated T cells (NFAT) and NF-κB were determined. The *O*-GlcNAcylation of GSK-3β, a negative regulator of NFAT, was significantly increased in *Ogt*-Tg mice, whereas the phosphorylation of GSK-3β was reciprocally reduced. The same result was observed for NF-κB p65. An in vitro reporter assay showed that the augmentation of *O*-GlcNAcylation by an *O*-GlcNAcase inhibitor suppressed NFAT and NF-κB promoter activity. These data suggest that augmented *O*-GlcNAcylation mitigates IH-induced cardiac remodeling by suppressing NFAT and NF-κB activities through the *O*-GlcNAcylation of GSK-3β and NF-κB p65.

Keywords *O*-GlcNAcylation · NFAT · NF-κB · GSK-3β · cardiac remodeling

Introduction

O-GlcNAcylation is a posttranslational modification of various proteins, and it was first described in the surface proteins of lymphocytes [1]. *O*-GlcNAcylation is catalyzed by two enzymes, *O*-GlcNAc transferase (OGT), which transfers *N*-acetylglucosamine (GlcNAc) from uridine diphospho (UDP)-GlcNAc to serine and threonine residues of acceptor proteins, and *O*-GlcNAcase (OGA), which removes GlcNAc from modified proteins [2]. Like phosphorylation, *O*-GlcNAcylation is one of the most-common posttranslational modifications. These two modifications have much in common; they both target serine and threonine residues of proteins [3] and are dynamically regulated by various cellular signals [4]. Several interactions between *O*-GlcNAcylation and phosphorylation, which can be

✉ Michio Asahi
masahi@osaka-med.ac.jp

[1] Department of Pharmacology, Osaka Medical College, Osaka, Japan

[2] Department of Cardiovascular Pharmacotherapy and Toxicology, Osaka University of Pharmaceutical Sciences, Osaka, Japan

[3] Department of Cardiovascular Medicine, Osaka City University Graduate School of Medicine, Osaka, Japan

[4] Department of Pharmacology, Osaka City University Graduate School of Medicine, Osaka, Japan

grouped into two representative types of interactions, have been reported: one is "competitive occupancy" at the same site, whereas the other is "alternative occupancy" at adjacent sites [2]. These interactions affect various cellular events.

Sleep apnea syndrome (SAS) manifests as recurrent episodes of hypoxemia and arousal during sleep and has been associated with heart failure (HF) in various studies [5]. Hypoxia has been shown to induce hemodynamic stress in HF patients. It has been reported that ischemic preconditioning [6] and ischemia/reperfusion (I/R)-induced stress elevate *O*-GlcNAcylation [7]. Hypoxia is often followed by deoxygenation and injures cardiomyocytes and damages cardiac function. Cardiac hypertrophy is one of the symptoms of hypoxia-exposed or pressure-loaded overworked hearts [8].

The role of *O*-GlcNAcylation in hypoxia is controversial. In isolated rat hearts, it has been reported that an increase in *O*-GlcNAcylation induced by glucosamine, an inducer of UDP-GlcNAc, or PUGNAc, an OGA inhibitor, protects heart function from I/R stress [9] and that azaserine, a UDP-GlcNAc synthesis pathway (HBP) inhibitor, exacerbates heart dysfunction [10]. In contrast, it has been reported that *O*-GlcNAcylation is increased in post-MI heart failure and thus leads to compromised cardiac contractility, showing a possible role for *O*-GlcNAcylation in the development of chronic cardiac dysfunction [11].

Inflammation is involved in the pathogenesis of numerous types of cardiovascular dysfunction, implying that *O*-GlcNAcylation modulates cardiac function via the regulation of inflammation [12]. In trauma-hemorrhagic shock model animals, glucosamine, one of the raw materials of UDP-GlcNAc, alleviates cardiac function through the attenuation of the NF-κB pathway, which is key for the regulation of inflammation.

Nuclear factor of activated T cells (NFAT) is phosphorylated and is predominantly located in the cytoplasm under normal conditions. Upon hypertrophic stimulation, NFAT is dephosphorylated by calcineurin, translocates into the nucleus, and then activates various hypertrophic genes [13]. Once activated, NFAT is then rephosphorylated by kinases such as c-JUN kinase and glycogen synthase kinase-3β (GSK-3β) before relocating to the cytoplasm.

Here, we studied the role of *O*-GlcNAcylation in intermittent hypoxia (IH)-induced cardiac hypertrophy using an IH mouse model. The results showed that augmented *O*-GlcNAcylation mitigated cardiac remodeling induced by 2 weeks of IH by suppressing NF-κB and NFAT activities. To gain insights into the molecular mechanisms, we examined the relationship between the phosphorylation and *O*-GlcNAcylation of NF-κB p65 and GSK-3β in vivo and the effects of *O*-GlcNAcylation on NF-κB and NFAT-promoter activities in HEK293T cells and/or H9c2 cells, a rat cardiomyoblast cell line, in vitro.

Materials and methods

Antibodies and reagents

An anti-*O*-GlcNAc antibody (RL-2), which detects *O*-GlcNAcylated proteins, was purchased from Novus Biologicals (Littleton, CO, USA). Anti-OGT, anti-OGA, and anti-NF-κB p65 antibodies were obtained from Santa Cruz Biotech (Dallas, Texas, USA). Anti-phospho-NF-κB p65 (Ser536), anti-phospho-GSK-3β (Ser9), and anti-GSK-3β antibodies were procured from Cell Signaling Technologies (Danvers, MA, USA). For cell culture experiments, a highly specific OGA inhibitor, Thiamet-G (TMG), an OGT inhibitor, benzyl-2-acetamido-2-deoxy-α-D-galactopyranoside (BADGP), and tumor necrosis factor α were obtained from Cayman Chemical (Ann Arbor, MI, USA), Sigma-Aldrich (St. Louis, MO, USA), and Wako Pure Chemical Industries, Ltd. (Osaka, Japan), respectively.

Mice

Ogt-Tg mice were generated as described previously [14]. We employed heterozygous *Ogt*-Tg (*Ogt*-Tg (+/−)) mice to evaluate the role of *O*-GlcNAcylation in IH. All studies on animal models were approved by the Ethical Committees of Animal Experiment of the Osaka Medical College (protocol #30059) and Osaka University of Pharmaceutical Sciences (protocol #24) and performed according to their guidelines.

IH

Wild-type (WT) and *Ogt*-Tg mice (male, 10–12 weeks) were exposed to IH as described previously [15]. In brief, a cycle of 5% O_2 for 1 min and 20% O_2 for 5 min was repeated for 8 h during the daytime each day. After 14 days of IH, the mice were anesthetized and killed for various analyses. Heart weight (Hw), body weight (Bw), and tibia length (TL) were measured, and the Hw/Bw and Hw/TL ratios were calculated for all mice.

Light microscopy

Cardiac tissues were fixed in 10% formaldehyde, embedded in paraffin, and cut into 4-μm sections. Photographs were taken at a magnification of × 4 and were transformed into binary images. The cardiac cross-sectional area was evaluated at a magnification of × 400 by a method reported previously [16]. After staining with Sirius Red, color images were randomly selected from five high-power fields

(at a magnification of × 200), and the collagen volume ratio (%) was calculated as described previously [17].

Echocardiographic measurement

Before and after the 2-week protocol of IH in WT and *Ogt*-Tg mice, transthoracic echocardiography was performed using a Vivid E9 instrument (GE Healthcare, Salt Lake City, UT, USA). The LV end-diastolic diameter (Dd) and the LV end-systolic diameter (Ds) were obtained based on M-mode measurements, and LV fractional shortening (FS) was calculated. The early LV filling velocity (E) and late diastolic filling (A) of mitral inflow were recorded in the apical four-chamber view, with the sample volume near the tips of the mitral leaflets at the site where velocity was maximal and flow was laminar. In addition, the early velocity (e′) of the mitral annulus was determined by tissue Doppler imaging, and the ratio of E to e′ (E/e′ ratio) was calculated. Furthermore, right ventricular global systolic function was evaluated by determining tricuspid annular plane systolic excursion (TAPSE).

Terminal deoxynucleotidyl transferase-mediated dUTP-biotin end labeling assay

A terminal deoxynucleotidyl transferase-mediated dUTP-biotin end labeling (TUNEL) assay was performed on myocardial tissue samples using an Apop Tag peroxidase in situ apoptosis detection kit (Millipore Japan, Tokyo, Japan). Negative control samples were incubated with distilled water, and the endometrium was used as a positive control. After counterstaining with Mayer's hematoxylin, TUNEL-positive cells were counted.

Immunohistochemical assessment of 4-hydroxy-2-nonenal protein expression

The levels of 4-hydroxy-2-nonenal (4-HNE)-modified protein adducts in ventricular paraffin sections were determined by immunohistochemical staining. Sections were incubated with a monoclonal antibody against 4-HNE (Japan Institute for the Control of Aging, Shizuoka, Japan) and a secondary antibody (biotinylated anti-mouse IgG), followed by incubation with Vectastain Elite ABC reagent (Vector Laboratories, Burlingame, CA, USA). The area (%) of 4-HNE staining was then quantified. To calculate the 4-HNE expression ratio, the mean control area (%) was defined as 1.0.

Cell culture

H9c2 cells, a rat cardiomyocyte-derived cell line, and HEK293T cells were purchased from the European Cell Culture Collection through DS Pharma Biomedical (Osaka, Japan) and the American Type Culture Collection, respectively. The cells were maintained in Dulbecco's Modified Eagle Medium (DMEM) with 10% fetal bovine serum containing 100 U/ml penicillin and 100 μg streptomycin in a CO_2 incubator (5% CO_2, 37 °C).

NF-κB reporter assay

NFAT reporter and CMV-renilla luciferase vectors (Promega, Madison, WI, USA) were transfected into the cells using Lipofectamine 2000 (Life Technologies, Carlsbad, CA, USA) according to the manufacturer's instructions. The transfected cells were incubated for 6 h either under normoxic conditions or in a hypoxic chamber (STEMCELL Technologies Inc., Vancouver, Canada) at 2% O_2 and 5% CO_2 with/without 20 ng/ml TNF-α. Luciferase activity was measured using a Dual-Glo assay system (Promega) with a GloMax-Multi Detection System (Promega) according to the manufacturer's instructions.

NFAT reporter assay

NFAT reporter and CMV-renilla luciferase vectors (Promega) were transfected into the cells using Lipofectamine 3000 (Life Technologies) according to the manufacturer's instructions. The transfected cells were incubated in a hypoxic chamber (STEMCELL Technologies Inc.) for 6 h at 37 °C. Luciferase activity was measured as described above.

Co-immunoprecipitation

The pCAGGS/*Ogt* plasmids were transfected into H9c2 cells using Lipofectamine 3000 (Life Technologies). The cells were exposed to IH (2% O_2 for 3 h twice with a period of normoxia for 3 h), lysed, and co-immunoprecipitated with Protein G magnetic beads (Bio-Rad, Hercules, CA, USA) that were preincubated with an anti-*O*-GlcNAc antibody. The immunoprecipitates were subjected to western blot analysis as described below.

Western blot analysis

The cell lysates were subjected to SDS-PAGE and then blotted onto a polyvinylidene difluoride membrane (Merck Millipore, Billericam, MA, USA) using a Trans-Blot system (Bio-Rad). The membrane was probed with appropriate primary and secondary horseradish peroxidase-conjugated antibodies after blocking with 5% skimmed milk and visualized using Luminata (Merck Millipore). Images were taken with ChemDoc XRS (Bio-Rad).

Quantitative reverse transcription PCR (qRT-PCR)

Total RNA was extracted from myocardial tissues and cells using TRI reagent (Molecular Research Center Inc., Cincinnati, OH, USA). Complementary DNA was synthesized from total RNA by reverse transcription using the Transcriptor Universal cDNA Master kit (Roche Diagnostics, Basel, Switzerland). mRNA levels were measured using a LightCycler (Roche Diagnostics), and the results were normalized to glyceraldehyde 3-phosphate dehydrogenase as an internal control.

Results

Effects of OGT overexpression and IH exposure on *O*-GlcNAcylation in the heart tissues of WT and *Ogt*-Tg mice

We first examined the alterations in OGT expression and *O*-GlcNAcylation levels in the hearts of WT and *Ogt*-Tg mice with/without IH. Under normoxic conditions, *O*-GlcNAcylation levels were higher in *Ogt*-Tg mice than in WT mice (Fig. 1a), as expected. After IH, *O*-GlcNAcylation was significantly increased in WT mice, indicating that IH elevates *O*-GlcNAcylation levels in heart tissues. Moreover, the IH-induced elevation of *O*-GlcNAcylation in *Ogt*-Tg mice was significantly higher than that in WT mice (Fig. 1a, b). In addition to *O*-GlcNAcylation, OGT expression increased after IH in WT mice (Fig. 1b). OGT expression levels were higher at the basal state in *Ogt*-Tg mice than in WT mice, as expected. After IH, the OGT expression in *Ogt*-Tg mice was even more increased than that in WT mice, and this was consistent with the *O*-GlcNAcylation level (Fig. 1b). Collectively, *O*-GlcNAcylation levels were synergistically increased in IH-exposed *Ogt*-Tg mice by both IH and the *Ogt* transgene.

IH-induced cardiac remodeling in WT and *Ogt*-Tg mice

As IH and the *Ogt* transgene affected the *O*-GlcNAcylation level in the heart tissues of mice, we examined the effects of *O*-GlcNAcylation on cardiac remodeling using WT and *Ogt*-Tg mice with/without IH. By gross pathology, WT mice exhibited an enlargement and increased wall thickness of both ventricles after IH, which is characteristic of concentric hypertrophy (Fig. 2a). The microscopic findings showed that cardiomyocytes were disarrayed and inflammatory cells were infiltrated (Fig. 2b). The average size of cardiomyocytes was significantly increased after IH in WT mice (Fig. 2c). In contrast, cardiac hypertrophy was not developed and cardiomyocytes were almost intact after IH in *Ogt*-Tg mice (Fig. 2a, b, c). As a major marker of maladaptive hypertrophy, cardiac fibrosis in cardiomyocytes was examined by Sirius Red staining. Fibrotic regions, which were Sirius Red-positive, were prominent, and these areas were increased around blood vessels after IH in WT mice, whereas they did not develop after IH in *Ogt*-Tg mice (Fig. 2d, e). Collectively, cardiac remodeling after IH was strongly reduced in *Ogt*-Tg mice, suggesting that *O*-GlcNAcylation might be protective against IH-induced cardiac maladaptive hypertrophy.

Estimation of LV function and remodeling with/without IH in WT and *Ogt*-Tg mice

Although there was no significant change in LV systolic function in WT mice with/without IH, IH significantly increased the ratios of E/A and E/e′, suggesting IH-induced diastolic dysfunction in WT mice (Fig. 3a). On the other hand, there were no significant changes in either systolic or diastolic function in *Ogt*-Tg mice with/without IH. Right ventricular function was evaluated by TAPSE and showed no significant change in either WT or *Ogt*-Tg mice with/without IH (Fig. 3a). The Hw/TL ratio significantly increased with IH in WT mice, whereas the increase was reversed in *Ogt*-Tg mice, although the Hw/Bw ratio did not increase with IH in WT and *Ogt*-Tg mice (Fig. 3b).

Apoptosis and lipid peroxidation with/without IH in the heart tissues of WT and *Ogt*-Tg mice

It has been reported that pathophysiological stresses such as IH perturb normal cell turnover, causing accelerated apoptosis compared with regeneration from circulating and cardiac progenitor cells [18]. Therefore, we evaluated the apoptosis of cardiomyocytes in WT and *Ogt*-Tg mice with/without IH. Under normoxic conditions, very few apoptotic cardiomyocytes were seen in both mouse strains (Fig. 4a), although a detailed calculation of TUNEL-positive cells revealed that the number of apoptotic cells was higher, although not significantly higher, in *Ogt*-Tg mice than in WT mice (Fig. 4a, b). Exposure to IH for 2 weeks significantly increased the number of TUNEL-positive apoptotic cells in WT mice. In contrast, no significant increase in apoptosis was observed in *Ogt*-Tg mice (Fig. 4a, b). We next examined whether IH induces lipid peroxidation in heart tissues. Under normoxic conditions, there were very few 4-HNE-positive cells the hearts of both WT and *Ogt*-Tg mice, whereas IH significantly elevated the number of 4-HNE-positive cells in WT mice (Fig. 4c, d). On the other hand, 4-HNE-positive

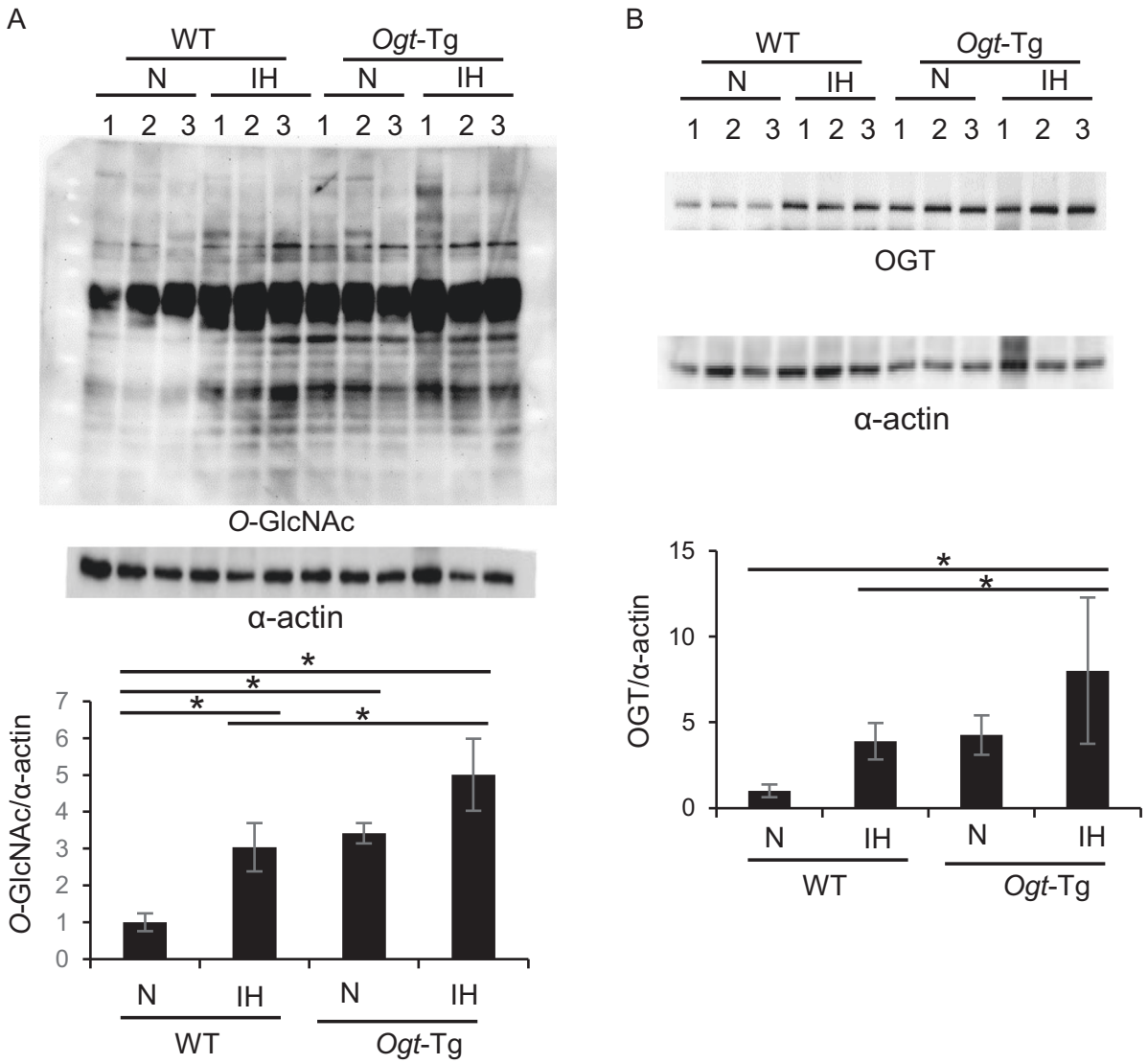

Fig. 1 Western blot analysis of heart tissues from WT and *Ogt*-Tg mice with/without IH. The expression levels of total protein *O*-GlcNAcylation **a** and OGT **b** were estimated in heart tissues from WT and *Ogt*-Tg mice under normoxic conditions (N) or after IH (IH). The band intensities were normalized to those of α-actin (lower panel). $^{*}p < 0.05$ with Tukey's test

cells were less relevant in the hearts of *Ogt*-Tg mice. These results suggest that OGT overexpression prevents IH-induced cardiac remodeling via the suppression of apoptosis or lipid peroxidation.

Effects of *O*-GlcNAcylation on NF-κB p65 phosphorylation in the heart tissues of WT and *Ogt*-Tg mice

It has been reported that the constitutively active state of the TNF-α/NF-κB pathway deteriorates cardiac function and that the inhibition of the pathway attenuates this dysfunction [19]. In this regard, we examined the phosphorylation of NF-κB p65 in the heart tissues of WT and *Ogt*-Tg mice. The ratio of phospho-NF-κB to total-NF-κB was calculated based on the Western blot band densities, indicating that the ratio was higher in WT mice than in *Ogt*-Tg mice (Fig. 5a). Upon exposure to IH, the ratio was slightly increased in WT mice but rather suppressed in *Ogt*-Tg mice (Fig. 5a).

Interaction between the *O*-GlcNAcylation and phosphorylation of NF-κB p65 in HEK293T cells

The phosphorylation of NF-κB p65 was significantly increased via IH, whereas the *O*-GlcNAcylation of NF-κB p65 was barely changed with/without IH.

However, OGT overexpression led to an obvious increase in *O*-GlcNAcylation and reversed the phosphorylation, whereas *O*-GlcNAcylated NF-κB p65 was

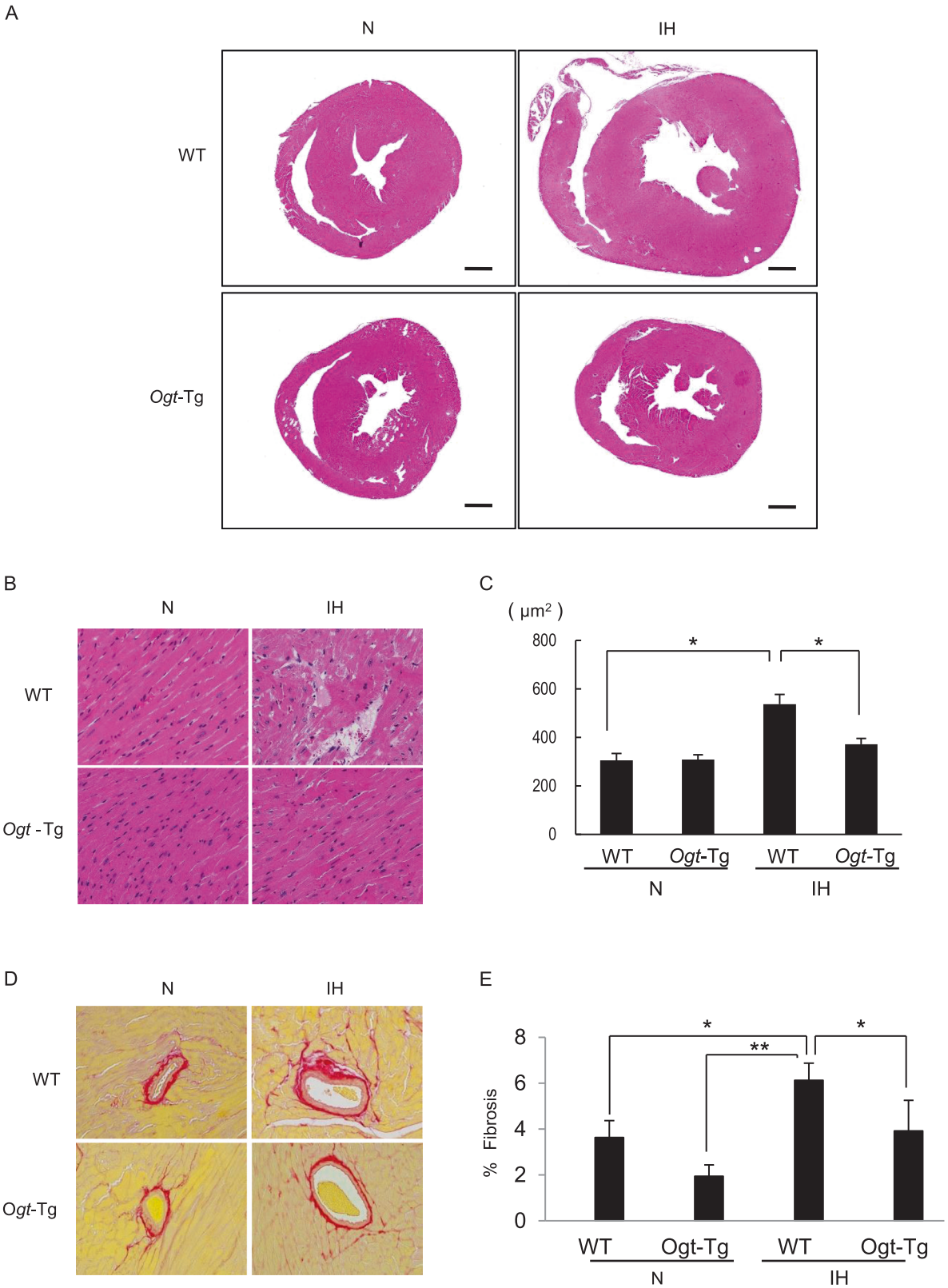

Fig. 2 Histological examination of LV myocardium from WT and *Ogt*-Tg mice exposed to IH. Samples of LV myocardium from WT and *Ogt*-Tg mice under normoxic conditions or after IH were examined histologically. **a** Cardiac cross-sections were stained using hematoxylin and eosin (H&E) (scale bars, 1 mm). **b** The cardiac tissue specimens stained with H&E were examined by light microscopy. **c** The average size of the cardiomyocytes was calculated with ImageJ. **d** Cardiac tissue specimens stained with Sirius Red were examined by light microscopy. **e** Collagen volume per total area was calculated and expressed as % fibrosis. $*p < 0.05$, $**p < 0.01$

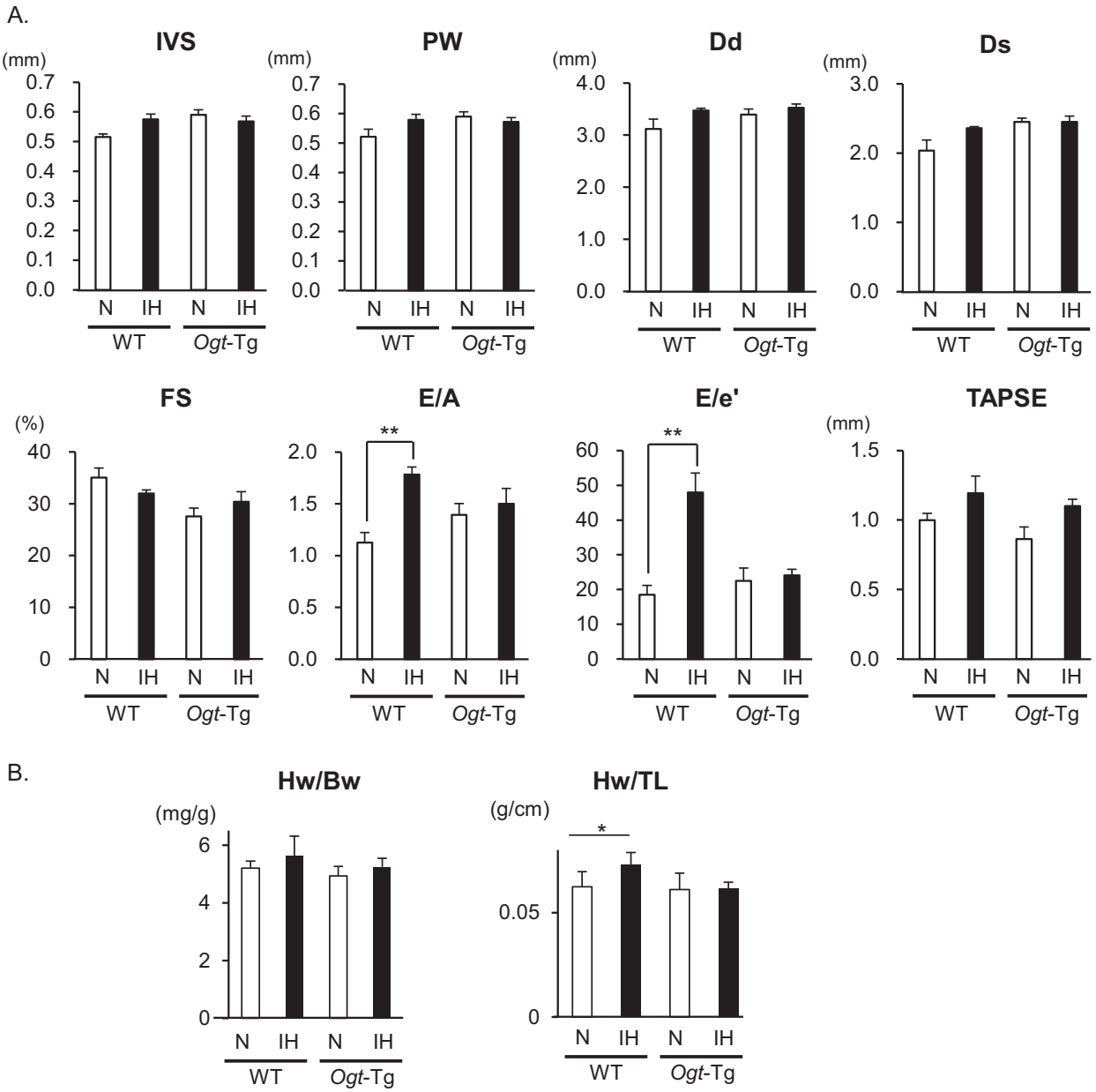

Fig. 3 Estimation of cardiac function and remodeling after IH in WT and *Ogt*-Tg mice. **a** Transthoracic echocardiography was performed in WT and *Ogt*-Tg mice under normoxic conditions or after exposure to a 2-week protocol of IH to measure the following parameters: interventricular septum (IVS), posterior left ventricle wall (PW), end-diastolic dimension (DD), internal dimension in systole (DS), fractional shortening (FS), the early LV filling velocity (E)/late diastolic filling (A) ratio of mitral inflow (E/A), the early LV filling velocity (E) of mitral inflow/early velocity (e′) of the mitral annulus ratio (E/e′), and tricuspid annual plane systolic excursion (TAPSE). $^{**}p < 0.01$. **b** Heart weight (Hw), body weight (Bw), and tibia length (TL) were measured, and the Hw/Bw and Hw/TL ratios were calculated for the same mouse groups. $^{*}p < 0.05$

increased in HEK293T cells (Fig. 5b), which was consistent with the in vivo data for *Ogt*-Tg mice.

Effects of *O*-GlcNAcylation on NF-κB promoter activity in HEK293T cells

To examine the mechanism by which IL-1β is down-regulated in *Ogt*-Tg mice after IH, we performed an NF-κB promoter reporter assay in HEK293T cells. NF-κB promoter activity was elevated upon the addition of 20 ng/ml TNF-α, and the activation was synergistic upon 6 h exposure to hypoxia (Fig. 5c). Notably, the activation was suppressed by 1 μM TMG in a dose-dependent manner (Fig. 5c). These results suggest that NF-κB activity may have a causative role in IH-induced cardiac hypertrophy and that augmented *O*-GlcNAcylation may reduce the activity, resulting in the prevention of remodeling.

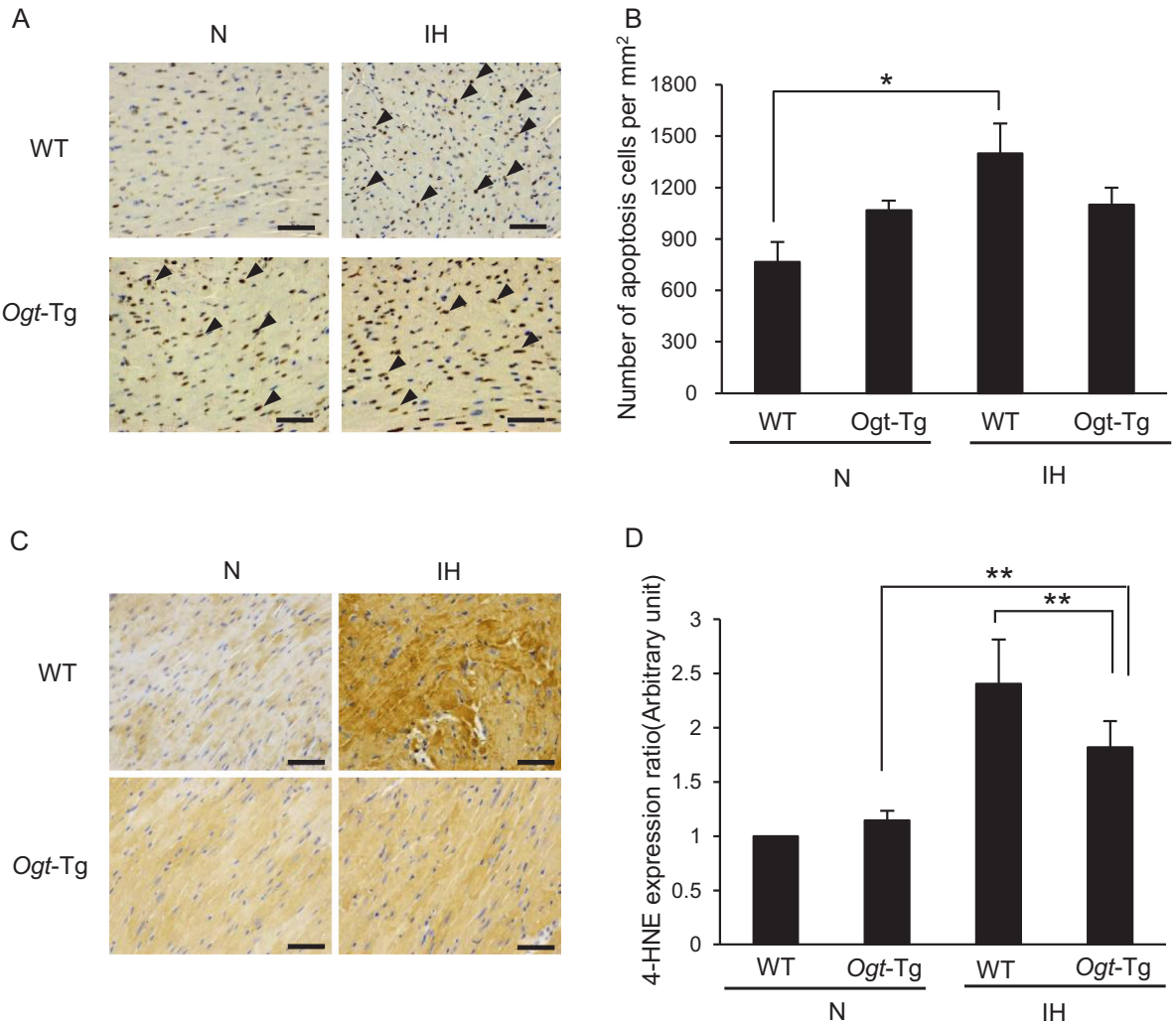

Fig. 4 TUNEL and 4-HNE staining of the myocardium under normoxic conditions or after IH in WT and *Ogt*-Tg mice. **a** TUNEL staining was performed on myocardial tissue samples under normoxic conditions or after IH in WT and *Ogt*-Tg mice. Negative control samples were incubated with distilled water, and the endometrium was used as the positive control. **b** After counterstaining with Mayer's hematoxylin, TUNEL-positive cells were counted as described previously. $*p < 0.01$. **c** The levels of 4-HNE-modified protein adducts in myocardial paraffin sections was determined by immunohistochemical staining. **d** The area (%) of 4-HNE staining was quantified. To calculate the 4-HNE expression ratio, the mean control area (%) was defined as 1.0. $**p < 0.05$

Effects of *O*-GlcNAcylation on the expression levels of IL-1β, BNP, and TGF-β in the heart tissues of WT and *Ogt*-Tg mice

To gain insight into the role of *O*-GlcNAcylation in cardiac remodeling, we performed qRT-PCR analysis using heart samples from WT or *Ogt*-Tg mice with/without IH. The inflammatory cytokine IL-1β was significantly increased in WT mice after IH, whereas it was unchanged in *Ogt*-Tg mice after IH (Fig. 5d, upper panel). A similar effect was observed for BNP (Fig. 5d, middle panel), a marker of cardiac function, and for TGF-β, a potent signaling molecule for fibrosis (Fig. 5d, lower panel), indicating that IH induces cardiac dysfunction with fibrosis in the heart tissues of WT mice and that remodeling does not occur in the heart tissues of *Ogt*-Tg mice. Taken together with the histological examination (Fig. 2) and echocardiography results (Fig. 3), our results suggest that augmented *O*-GlcNAcylation strongly inhibits cardiac hypertrophy with fibrosis and diastolic dysfunction induced by IH.

Effects of *O*-GlcNAcylation on GSK-3β phosphorylation in the heart tissues of WT and *Ogt*-Tg mice

It is well known that the transcription factor NFAT is a key regulator of cardiac hypertrophy [20]. The dephosphorylation of NFAT by phosphatases such as calcineurin induces its nuclear translocation and transactivates various genes, inducing cardiac hypertrophy. Conversely,

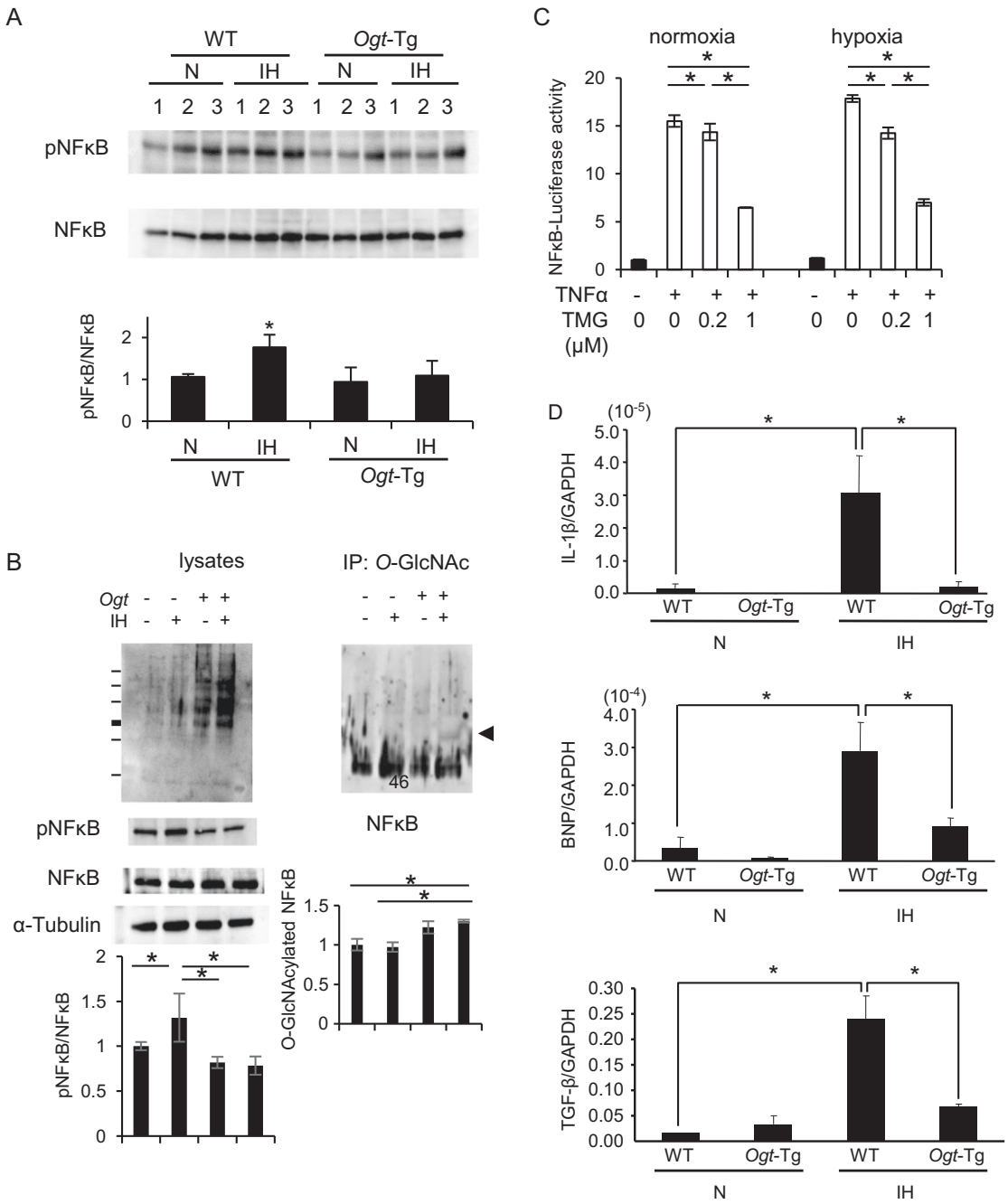

Fig. 5 Effects of *O*-GlcNAcylation on NF-κB p65 phosphorylation, NF-κB promoter activity, and mRNA levels of IL-1β, BNP, and TGF-β. **a**, **b** Western blot analysis of NF-κB phosphorylation. The phosphorylation of NF-κB **a** in the heart tissues of WT and *Ogt*-Tg mice under normoxic conditions or after exposure to the 2-week protocol of IH and **b** in 293 T cells with/without *Ogt* transfection and with/without exposure to IH (2% O_2 for 3 h twice with a period of normoxia for 3 h) was evaluated by western blot analysis. The arrowhead indicates *O*-GlcNAcylated NF-κB. $^*p < 0.05$ with Tukey's test. **c** NF-κB reporter assay in 293 T cells. The cells were treated with 20 ng/ml TNFα ± TMG (0.2 or 1 μM) either under normoxia or hypoxia (2% O_2, 5% CO_2) for 6 h, and then NF-κB-luciferase activity was measured. $^*p < 0.05$ with Tukey's test. **d** Quantitative RT-PCR analysis of heart samples from WT and *Ogt*-Tg mice. Total RNA was extracted from the myocardial tissues of WT or *Ogt*-Tg mice under normoxic conditions or after exposure to the 2-week protocol of IH. After the mRNA levels of IL-1β, BNP, and TGF-β were measured, the results were normalized to GAPDH as an internal control. $^*p < 0.05$: Student's *t* test

several kinases phosphorylate NFAT, inhibiting nuclear translocation. GSK-3β is one such kinase that negatively regulates NFAT activity. We then examined the phosphorylation of GSK-3β in the heart tissues of WT and *Ogt*-Tg mice. Under normoxic conditions, the phosphorylation of GSK-3β was slightly lower in *Ogt*-Tg mice than

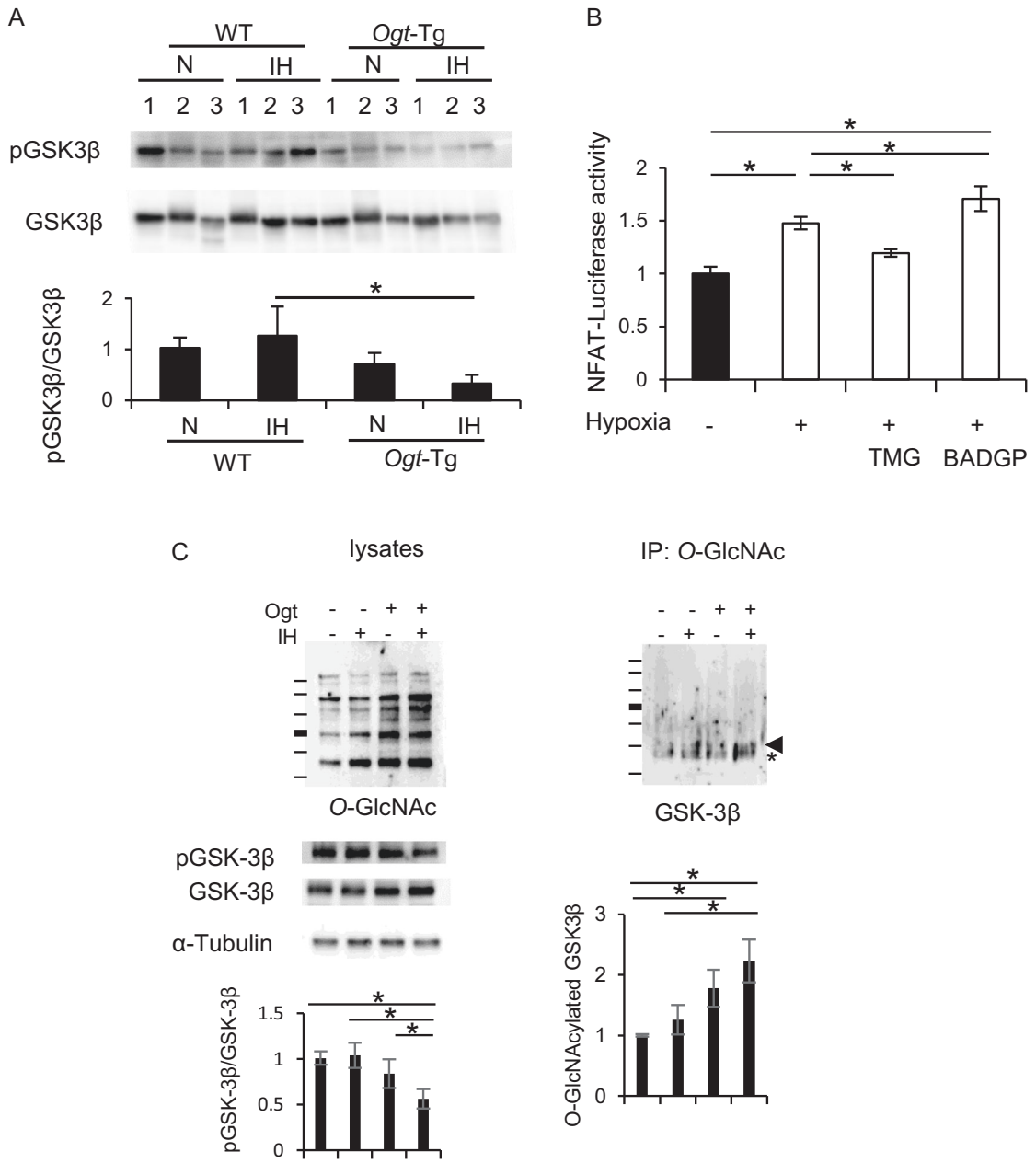

Fig. 6 Phosphorylation/*O*-GlcNAcylation of GSK-3β and NFAT reporter assay. **a** The phosphorylation of GSK-3β in WT and *Ogt*-Tg mice exposed to IH was evaluated by western blot analysis. All bands were densitometrically analyzed, and the pGSK-3β to GSK-3β ratio was calculated. *$p < 0.05$ with Tukey's test. **b** NFAT reporter assay in H9c2 cells. The cells were cultured with/without exposure to hypoxia for 6 h in the presence or absence of 1 μM TMG or 16 μM BADGP, and NFAT-luciferase activity was measured. *$p < 0.05$ with Tukey's test. **c** The *O*-GlcNAcylation of GSK-3β in H9c2 cells exposed to IH. The OGT expression vector was transfected into H9c2 cells. The cells were exposed to IH (2% O_2 for 3 h twice with a period of normoxia for 3 h) and then lysed. The cell lysates were immunoprecipitated with an anti-*O*-GlcNAc antibody, and the precipitates were subjected to Western blot analysis. *$p < 0.05$ with Tukey's test

in WT mice. Unphosphorylated GSK-3β levels were significantly elevated in the hearts of *Ogt*-Tg mice upon exposure to IH, whereas IH did not affect the phosphorylation of GSK-3β in WT mice (Fig. 6a). Because unphosphorylated GSK-3β is the active form, it is implied that GSK-3β is activated in the heart tissues of *Ogt*-Tg mice, but not WT mice, after IH.

Effects of *O*-GlcNAcylation on NFAT-promoter activity in H9c2 cells

To examine the direct effects of *O*-GlcNAcylation on NFAT-promoter activity, we exploited an NFAT-promoter luciferase assay using H9c2 cells. As expected, exposure to hypoxia for 6 h increased luciferase activity in H9c2 cells

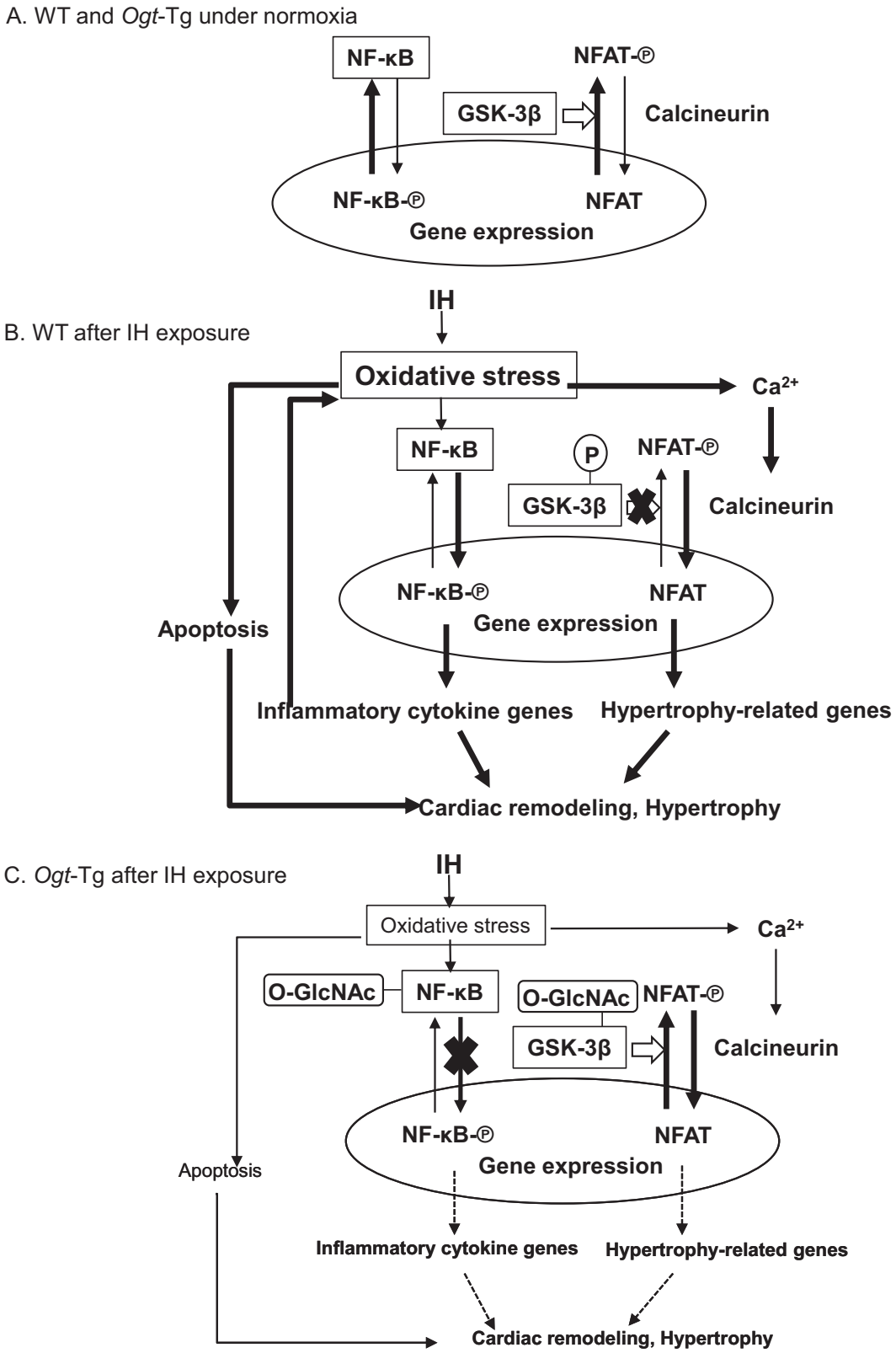

(Fig. 6b). Augmented *O*-GlcNAcylation induced by 1 μM TMG significantly suppressed NFAT-luciferase activity in H9c2 cells. In contrast, the addition of 36 μM BADGP, an inhibitor of OGT [21], enhanced NFAT-luciferase activity. These results suggest that *O*-GlcNAcylation can attenuate hypoxia-induced NFAT activation. We next evaluated

◀ **Fig. 7** Possible mechanism by which IH-induced cardiac remodeling is attenuated in *Ogt*-Tg mice. The mechanism by which IH-induced cardiac remodeling is attenuated in *Ogt*-Tg mice are shown schematically. **a** WT and *Ogt*-Tg heart tissues under normoxic conditions. The transcriptional factors NF-κB and NFAT are not activated under normoxic conditions. **b** WT heart tissues after IH. Increased oxidative stress after IH activates NF-κB to induce inflammatory cytokines and subsequently increases intracellular calcium, activating NFAT via calcineurin. By activating two transcriptional factors related to cardiac remodeling, the cardiac muscle becomes thick and fibrotic. **c** *Ogt*-Tg mouse heart tissues after IH. The phosphorylation of NF-κB p65 and GSK-3β is inhibited by the augmentation of *O*-GlcNAcylation in *Ogt*-Tg. Reduced phosphorylation inhibits the nuclear translocation of both NF-κB and NFAT, resulting in a reduction in cardiac remodeling

whether the reduction in unphosphorylated GSK-3β was attributed to the increase in *O*-GlcNAcylation. *Ogt*-transfected H9c2 cells exhibited higher *O*-GlcNAcylation than intact H9c2 cells (Fig. 6c). Exposure to IH increased overall protein *O*-GlcNAcylation, whereas the phosphorylation of GSK-3β was unchanged. In contrast, phosphorylation was suppressed in *Ogt*-transfected cells, and the suppression was significantly strengthened by IH. The *O*-GlcNAcylation of GSK-3β, which was promoted by IH, was also increased significantly in *Ogt*-transfected cells, although this increase was not significant. (Fig. 6c). The activation of GSK-3β, that is, the increase in unphosphorylated GSK-3β, may be due to the *O*-GlcNAcylation of GSK-3β. These results suggest that augmented *O*-GlcNAcylation increases *O*-GlcNAcylated GSK-3β and then increases unphosphorylated GSK-3β, the active form, resulting in NFAT inactivation.

Discussion

Both Type 2 diabetes mellitus (T_2DM) and SAS have been reported to be associated with the progression of cardiac remodeling followed by heart failure [5, 6]. As there is a bidirectional relationship between SAS and T_2DM [22], we focused on *O*-GlcNAcylation, which is elevated in T_2DM, to examine the effects of T_2DM on the progression of cardiac remodeling in an IH mouse model. Here, we showed that augmented *O*-GlcNAcylation mitigated the cardiac remodeling induced by 2 weeks of IH. To clarify the mechanism, we examined the activities of the major transcriptional factors involved in cardiac remodeling, namely, NF-κB and NFAT, in WT and *Ogt*-Tg heart tissues. The possible mechanisms are represented schematically in Fig. 7. In brief, after IH, increased oxidative stress activates NF-κB to induce inflammatory cytokines, and a subsequent increase in intracellular calcium activates NFAT in WT heart tissue. The activation of the two transcriptional factors induces cardiac muscle to become thick and fibrotic. In contrast, the augmentation of *O*-GlcNAcylation in *Ogt*-Tg heart tissues is even more increased after IH. As a result, the *O*-GlcNAcylation of NF-κB p65 and GSK-3β is elevated, resulting in the inhibition of their phosphorylation. This reduced phosphorylation inhibits the nuclear translocation of both NF-κB and NFAT, resulting in reduced cardiac remodeling.

Both NFAT and NF-κB are Rel homology domain-containing transcription factors, and their independent activities are critically involved in regulating cardiac hypertrophy [23]. In vitro experiments using H9c2 cells showed that GSK-3β phosphorylation and the activation of NFAT transcriptional activity are upregulated after hypoxia (Fig. 6b). NFAT activation may be involved in IH-induced hypertrophy. Reactive oxygen species (ROS), including superoxides, have emerged as important molecules in cardiac hypertrophy. GPCR agonist-induced cardiac hypertrophy is mediated through NF-κB activation via the generation of ROS [24]. In our IH mouse model, it was shown that ROS are increased after 2 weeks of IH and that the inhalation of H_2 gas is effective in preventing left ventricular (LV) remodeling induced by IH [25]. Moreover, in vitro experiments using HEK293T cells showed that NF-κB transcriptional activity is activated after hypoxia treatment (Fig. 3d). Collectively, NF-κB activation via the generation of ROS may also be involved in IH-induced hypertrophy as well as GPCR agonist-induced hypertrophy.

In diabetic patients, elevated glucose increases flux through the HBP [26], which often leads to increased concentrations of UDP-GlcNAc. UDP-GlcNAc is the donor substrate for *O*-GlcNAcylation. It is thought that diabetic complications such as retinopathy [27], nephropathy [28], and cardiomyopathy [29] are partly owing to augmented *O*-GlcNAcylation. Surprisingly, we showed here that augmented *O*-GlcNAcylation attenuated IH-induced cardiac remodeling, hypertrophy, and fibrosis. Given that T_2DM deteriorates SAS-induced cardiac remodeling in clinical settings, we expected that cardiac remodeling would be promoted in the heart tissues of *Ogt*-Tg mice. However, unexpectedly, augmented *O*-GlcNAcylation attenuated IH-induced cardiac remodeling. This paradox may be explained by the period of exposure to IH. Cardiac hypertrophy and fibrosis were significantly attenuated in *Ogt*-Tg hearts following 2 weeks of IH. In contrast, both systolic and diastolic functions were not changed in *Ogt*-Tg hearts, although diastolic function was significantly reduced in WT hearts. Diabetic cardiomyopathy is thought to be induced by the chronic augmentation of *O*-GlcNAcylation. Therefore, the 2 weeks period of IH was too short to observe the chronic effect. Angina pectoris rather than SAS may occur upon exposure to a short period of IH. Augmented *O*-GlcNAcylation might reduce cardiac remodeling in patients with angina pectoris. It is interesting to know how cardiac function is changed in *Ogt*-Tg mice if IH exposure

continues for longer periods. If it is attenuated in *Ogt*-Tg mice compared to WT mice, augmented *O*-GlcNAcylation in T_2DM may worsen SAS-induced cardiac dysfunction. Further study is required to elucidate the long-term effects of *O*-GlcNAcylation on IH-induced cardiac remodeling and dysfunction.

To examine the mechanism through which cardiac remodeling is attenuated in *Ogt*-Tg mice, we focused on the effects of *O*-GlcNAcylation on two related transcriptional factors, NFAT and NF-κB. As GSK-3β, which phosphorylates NFAT to induce a reduction in transcriptional activity, is known as one of the substrates of OGT [30], we examined the levels of *O*-GlcNAcylated and phosphorylated GSK-3β after 2 weeks of IH. The results showed that the *O*-GlcNAcylation of GSK-3β was increased and that phosphorylation was reduced reciprocally. Unphosphorylated GSK-3β phosphorylates NFAT, attenuating nuclear translocation to downregulate transcriptional activity. Regarding another transcriptional factor associated with cardiac remodeling, NF-κB, we also showed that the *O*-GlcNAcylation of NF-κB p65 attenuates its transcriptional activity through a reduction in NF-κB p65 phosphorylation. Thus, augmented *O*-GlcNAcylation attenuates IH-induced cardiac remodeling through the downregulation of the transcriptional activities of NFAT and NF-κB. SAS is known to activate the renin–angiotensin system and adrenergic nerves, which may promote cardiac remodeling. Because we did not expect that *O*-GlcNAcylation would affect the renin–angiotensin system and adrenergic nerves, it was not evaluated in this paper. The relationship between *O*-GlcNAcylation and the renin–angiotensin system or adrenergic nerves should be examined in the future.

In conclusion, we have revealed that augmented *O*-GlcNAcylation attenuates IH-induced maladaptive cardiac remodeling by reducing the transcriptional activities of NFAT and NF-κB by reducing the phosphorylation of GSK-3β and NF-κB p65.

Acknowledgements We are grateful to Mizuho Sasaki, Akira Watanabe, Takumi Noda, Mari Yamashita, Shota Tanikawa, Saki Morita (Osaka University of Pharmaceutical Sciences), Chieko Ohta, Yumiko Ogami, Nozomi Tokuhara, and Naoko Segawa (Osaka Medical College) for their expert technical assistance. This study was partially supported by the grant-in-aid for Scientific Research (C) no. 17590249 from the Japan Society for the Promotion of Science (M.A.) under the Ministry of Education, Science, Culture, Sports, and Technology of Japan.

Compliance with ethical standards

Conflict of interest The authors declare that they have no conflict of interest.

References

1. Torres CR, Hart GW. Topography and polypeptide distribution of terminal N-acetylglucosamine residues on the surfaces of intact lymphocytes. Evidence for O-linked GlcNAc. J Biol Chem. 1984;2595:3308–17.
2. Hart GW, Housley MP, Slawson C. Cycling of O-linked β-N-acetylglucosamine on nucleocytoplasmic proteins. Nature. 2007;4467139:1017–22.
3. Hart GW, Greis KD, Dong LY, Blomberg MA, Chou TY, Jiang MS et al. O-linked N-acetylglucosamine: the "yin-yang" of Ser/Thr phosphorylation? Nuclear and cytoplasmic glycosylation. Adv Exp Med Biol. 1995;376:115–23.
4. Kamemura K, Hart GW. Dynamic interplay between O-glycosylation and O-phosphorylation of nucleocytoplasmic proteins: a new paradigm for metabolic control of signal transduction and transcription. Prog Nucleic Acid Res Mol Biol. 2003;73:107–36.
5. Lanfranchi PA, Somers VK, Braghiroli A, Corra U, Eleuteri E, Giannuzzi P. Central sleep apnea in left ventricular dysfunction: prevalence and implications for arrhythmic risk. Circulation. 2003;1075:727–32.
6. Jensen RV, Johnsen J, Kristiansen SB, Zachara NE, Bøtker HE. Ischemic preconditioning increases myocardial O-GlcNAc glycosylation. Scand Cardiovasc J. 2013;473:168–74.
7. Champattanachai V, Marchase RB, Chatham JC. Glucosamine protects neonatal cardiomyocytes from ischemia-reperfusion injury via increased protein O-GlcNAc and increased mitochondrial Bcl-2. Am J Physiol Cell Physiol. 2008;2946:C1509–20.
8. Genovese A, Chiariello M, Cacciapuoti AA, De Alfieri W, Latte S, Condorelli M. Inhibition of hypoxia-induced cardiac hypertrophy by verapamil in rats. Basic Res Cardiol. 1980;756:757–63.
9. Liu J, Marchase RB, Chatham JC. Increased O-GlcNAc levels during reperfusion lead to improved functional recovery and reduced calpain proteolysis. Am J Physiol Heart Circ Physiol. 2007;2933:H1391–9.
10. Liu J, Pang Y, Chang T, Bounelis P, Chatham JC, Marchase RB. Increased hexosamine biosynthesis and protein O-GlcNAc levels associated with myocardial protection against calcium paradox and ischemia. J Mol Cell Cardiol. 2006;402:303–12.
11. Lunde IG, Aronsen JM, Kvaløy H, Qvigstad E, Sjaastad I, Tønnessen T et al. Cardiac O-GlcNAc signaling is increased in hypertrophy and heart failure. Physiol Genomics. 2012;442:162–72.
12. Ngoh GA, Facundo HT, Zafir A, Jones SP. O-GlcNAc signaling in the cardiovascular system. Circ Res. 2010;1072:171–85.
13. Wilkins BJ, Molkentin JD. Calcium–calcineurin signaling in the regulation of cardiac hypertrophy. Biochem Biophys Res Commun. 2004;3224:1178–91.
14. Moriwaki K, Asahi M. Augmented TME O-GlcNAcylation Promotes Tumor Proliferation through the Inhibition of p38 MAPK. Mol Cancer Res. 2017;159:1287–98.
15. Nishioka S, Yoshioka T, Nomura A, Kato R, Miyamura M, Okada Y et al. Celiprolol reduces oxidative stress and attenuates left ventricular remodeling induced by hypoxic stress in mice. Hypertens Res. 2013;36:934.
16. Kato R, Nomura A, Sakamoto A, Yasuda Y, Amatani K, Nagai S et al. Hydrogen gas attenuates embryonic gene expression and prevents left ventricular remodeling induced by intermittent hypoxia in cardiomyopathic hamsters. Am J Physiol Heart Circ Physiol. 2014;30711:H1626–H1633.
17. Yamashita C, Hayashi T, Mori T, Tazawa N, Kwak C-J, Nakano D et al. Angiotensin II receptor blocker reduces oxidative stress and attenuates hypoxia-induced left ventricular remodeling in apolipoprotein e–knockout mice. Hypertens Res. 2007;30:1219.

18. Anversa P, Kajstura J, Leri A, Bolli R. Life and death of cardiac stem cells: a paradigm sahift in cardiac biology. Circulation. 2006;11311:1451–63.
19. Kawamura N, Kubota T, Kawano S, Monden Y, Feldman AM, Tsutsui H et al. Blockade of NF-kappaB improves cardiac function and survival without affecting inflammation in TNF-alpha-induced cardiomyopathy. Cardiovasc Res. 2005;663:520–9.
20. Molkentin JD. Calcineurin–NFAT signaling regulates the cardiac hypertrophic response in coordination with the MAPKs. Cardiovasc Res. 2004;633:467–75.
21. Pantaleon M, Tan HY, Kafer GR, Kaye PL. Toxic effects of hyperglycemia are mediated by the hexosamine signaling pathway and O-linked glycosylation in early mouse embryos. Biol Rep. 2010;824:751–8.
22. Martinez Ceron E, Casitas Mateos R, Garcia-Rio F. Sleep apnea-hypopnea syndrome and type 2 diabetes. A reciprocal relationship? Arch Bronconeumol. 2015;513:128–39.
23. Liang Q, Bueno OF, Wilkins BJ, Kuan CY, Xia Y, Molkentin JD. c-Jun N-terminal kinases (JNK) antagonize cardiac growth through cross-talk with calcineurin–NFAT signaling. EMBO J. 2003;2219:5079.
24. Hirotani S, Otsu K, Nishida K, Higuchi Y, Morita T, Nakayama H et al. Involvement of nuclear factor-kappaB and apoptosis signal-regulating kinase 1 in G-protein-coupled receptor agonist-induced cardiomyocyte hypertrophy. Circulation. 2002;1054:509–15.
25. Hayashi T, Yoshioka T, Hasegawa K, Miyamura M, Mori T, Ukimura A et al. Inhalation of hydrogen gas attenuates left ventricular remodeling induced by intermittent hypoxia in mice. Am J Physiol Heart Circ Physiol. 2011;3013:H1062–9.
26. Marshall S, Bacote V, Traxinger RR. Discovery of a metabolic pathway mediating glucose-induced desensitization of the glucose transport system. Role of hexosamine biosynthesis in the induction of insulin resistance. J Biol Chem. 1991; 2668:4706–12.
27. Gurel Z, Sieg KM, Shallow KD, Sorenson CM, Sheibani N. Retinal O-linked N-acetylglucosamine protein modifications: implications for postnatal retinal vascularization and the pathogenesis of diabetic retinopathy. Mol Vis. 2013;19:1047–59.
28. Park MJ, Kim DI, Lim SK, Choi JH, Han HJ, Yoon KC et al. High glucose-induced O-GlcNAcylated carbohydrate response element-binding protein (ChREBP) mediates mesangial cell lipogenesis and fibrosis: the possible role in the development of diabetic nephropathy. J Biol Chem. 2014;28919:13519–30.
29. Yokoe S, Asahi M, Takeda T, Otsu K, Taniguchi N, Miyoshi E et al. Inhibition of phospholamban phosphorylation by O-GlcNAcylation: implications for diabetic cardiomyopathy. Glycobiology. 2010;2010:1217–26.
30. Shi J, Wu S, Dai CL, Li Y, Grundke-Iqbal I, Iqbal K et al. Diverse regulation of AKT and GSK-3beta by O-GlcNAcylation in various types of cells. FEBS Lett. 2012;58616:2443–50.